TWO-COMPONENT JET MODELS OF GAMMA-RAY BURST SOURCES

FANG PENG,[1] ARIEH KÖNIGL,[1] AND JONATHAN GRANOT[2]
Draft version January 2, 2008

ABSTRACT

Recent observational and theoretical studies have raised the possibility that the collimated outflows in gamma-ray burst (GRB) sources have two distinct components: a narrow (opening half-angle $\theta_{\rm j,n}$), highly relativistic (initial Lorentz factor $\eta_{\rm n} \gtrsim 10^2$) outflow, from which the γ-ray emission originates, and a wider ($\theta_{\rm j,w} \lesssim 3\,\theta_{\rm j,n}$), moderately relativistic ($\eta_{\rm w} \sim 10$) surrounding flow. Using a simple synchrotron emission model, we calculate the R-band afterglow lightcurves expected in this scenario and derive algebraic expressions for the flux ratios of the emission from the two jet components at the main transition times in the lightcurve. For viewing angles $\theta_{\rm obs} < \theta_{\rm j,n}$ we find that the contribution of the wide component to the optical afterglow is negligible if its kinetic energy $E_{\rm w}$ is significantly smaller than that of the narrow component, $E_{\rm n}$, as expected for the jet core and cocoon outflow components in the collapsar jet-breakout model. However, if $E_{\rm w}/E_{\rm n} > 1$ [but the isotropic-equivalent energy ratio $E_{\rm iso,w}/E_{\rm iso,n} = (E_{\rm w}/E_{\rm n})(\theta_{\rm j,n}/\theta_{\rm j,w})^2$ remains < 1], as expected for the decoupled neutron and proton components, respectively, in an initially neutron-rich, hydromagnetically accelerated jet model, then the narrow component only dominates the early afterglow and the wide component takes over after its nominal deceleration time $t_{\rm dec,w}$ (typically $\sim 0.1 - 1$ days). Given that $t_{\rm dec,w}$ is comparable to the jet-break time $t_{\rm jet,n}$ of the narrow component for characteristic parameter values, the emergence of the wide component at $t_{\rm dec,w}$ may mask the jet break in the narrow component at $t_{\rm jet,n}$, which in turn may lead to an overestimate of the γ-ray energy emitted by the source and hence of the required γ-ray emission efficiency. We apply this scheme also to X-ray flash sources, which we interpret as GRB jets viewed at an angle $\theta_{\rm obs} > \theta_{\rm j,n}$. Finally, we argue that a neutron-rich hydromagnetic outflow may naturally give rise to repeated brightening episodes in the afterglow lightcurve as observed in GRB 021004 and GRB 030329.

Subject headings: gamma rays: bursts — ISM: jets and outflows — radiation mechanisms: nonthermal

1. INTRODUCTION

Gamma-ray bursts (GRBs) and their afterglows are commonly interpreted in terms of a relativistic outflow that emanates from the vicinity of a solar-mass neutron star or black hole (e.g., Piran 1999; Mészáros 2002). In this picture, the prompt gamma-ray emission is attributed to a highly relativistic ejecta (with an initial Lorentz factor $\gamma \gtrsim 10^2$), whereas the subsequent afterglow emission in the X-ray, optical, and radio (over hours, days, and weeks, respectively, after the GRB) arises from the shock that is driven into the ambient medium as the ejecta sweeps up the external medium and decelerates. Most afterglow observations to date have been carried out hours to days after the GRB event, by which time the Lorentz factor of the afterglow shock has decreased to $\lesssim 10$. These observations have revealed the presence of achromatic breaks in the afterglow lightcurves of many sources, which strongly indicate that GRB outflows are collimated into narrow jets (Rhoads 1999; Sari et al. 1999).

Recently, however, the possibility that at least some GRB outflows consist of two distinct components has been raised in the literature. On the observational side, this possibility was first invoked by Pedersen et al. (1998), who suggested that the afterglow from GRB 970508 could be explained in terms of a narrow jet surrounded by an isotropic outflow. Frail et al. (2000) subsequently proposed that the γ-rays and early (shorter-wavelength) afterglow emission in GRB 991216 could be attributed to a narrow, ultrarelativistic outflow component, and that the late (longer-wavelength) afterglow emission in this source originates in a separate wide component that is only mildly relativistic. A similar picture was proposed for GRB 030329 by Berger et al. (2003b) and Sheth et al. (2003). A two-component model was also suggested as an explanation of the observed rebrightening of the X-ray flash (XRF) source XRF 030723 (Huang et al. 2004) as well as of the apparent peak-energy distribution of GRBs and XRFs (Liang & Dai 2004) and of the origin of the blueshifted optical absorption features in the spectrum of the GRB 021004 afterglow (Starling et al. 2005).

The possibility of a two-component outflow in GRB sources has been independently indicated by theoretical considerations. One can broadly divide the physical models that give rise to such an outflow into two classes: models in which the separation into two components is an intrinsic property of the outflow, and those in which a narrow relativistic jet gives rise to a wider and slower component as it propagates through (and interacts with) the envelope of a progenitor massive star. One example of a model of the first type was worked out by Levinson & Eichler (1993) and van Putten & Levinson (2003): it consists of (1) a relativistic, baryon-poor jet driven electromagnetically along disk-anchored magnetic field lines that thread the horizon of a rotating black hole,

[1] Department of Astronomy & Astrophysics and Enrico Fermi Institute, University of Chicago, 5640 South Ellis Avenue, Chicago, IL 60637; fpeng@oddjob.uchicago.edu, arieh@jets.uchicago.edu.
[2] Kavli Institute for Particle Astrophysics and Cosmology, Stanford University, P.O. Box 20450, MS 29, Stanford, CA 94309; granot@slac.stanford.edu.

and (2) a subrelativistic, baryon-rich wind that is driven thermally from that disk. Another example is provided by hydromagnetically driven jets that originate from a neutron star or a neutron-rich accretion disk that form in the collapse of a massive star (Vlahakis et al. 2003). In this case the neutrons decouple at a moderate Lorentz factor while the protons continue to be accelerated and collimated by the electromagnetic forces, giving rise to a narrow, highly relativistic proton component and a wider and slower neutron component (which, after decoupling, is transformed into a moderately relativistic proton component through neutron decay). Examples of models of the second type include jet-induced core-collapse supernovae, wherein collimated high-velocity jets cause the envelope of the progenitor massive star through which they propagate to be ejected with subrelativistic speeds and an oblate geometry (Khokhlov et al. 1999), and the collapsar model, in which the outflow resulting from the jet breakout through the progenitor star's envelope is predicted to consist of a highly relativistic jet core and a moderately relativistic surrounding cocoon (W. Zhang et al. 2004; see also Ramirez-Ruiz et al. 2002).

In this paper we focus on two-component GRB outflows in which both components initially move with relativistic speeds and therefore end up contributing to the optical afterglow emission. Accordingly, we adopt as representative examples the hydromagnetically accelerated, initially neutron-rich jet model of Vlahakis et al. (2003) and the collapsar jet-breakout model of W. Zhang et al. (2004). According to the numerical simulations of the latter authors, the narrow component in the collapsar model has a Lorentz factor $\eta_n \gtrsim 100$ and an opening half-angle $\theta_{j,n} \sim 3°–5°$, whereas the corresponding quantities for the wide component are $\eta_w \sim 15$ and $\theta_{j,w} \sim 10°$, respectively. The characteristic Lorentz factors in this scenario are very similar to those ($\eta_n \sim 200$ and $\eta_w \sim 15$) in the representative neutron-rich hydromagnetic model of Vlahakis et al. (2003).[3] However, *in contrast* with the collapsar model, in which the highly relativistic jet component is in general more energetic (typically by about an order of magnitude) than the cocoon material, the asymptotic kinetic energy E_w of the wide component in the hydromagnetic jet model typically exceeds the corresponding energy of the narrow component ($E_w \approx 2\,E_n$ in the fiducial model of Vlahakis et al. 2003).

Our goal in the present work is to examine some of the observational properties of two-component GRB outflows. In particular, we calculate (§ 2) the approximate optical afterglow lightcurves that are produced by the shocks that the two jet components would drive into the ambient medium. We then argue (§ 3) that outflows of this type may have significant general implications to our understanding of GRB and XRF sources. Our conclusions are given in § 4.

2. MODEL AFTERGLOW LIGHTCURVES

A simple jet structure is assumed in this work, consisting of a narrow and initially faster component and a wide and initially slower component. Each compo-

nent is assumed to be uniform within some finite opening angle and to have sharp edges. This two-component model should not be regarded as a limiting case of the structured "universal" jet models discussed in the literature (e.g., Rossi et al. 2002; Zhang & Mészáros 2002; B. Zhang et al. 2004). In the latter models, all jets are nearly identical and their injected energy per unit solid angle has a power-law or a Gaussian dependence on the polar angle θ (measured with respect to the jet axis). In contrast, in the scenario that we consider the wide component does not contribute to the γ-ray emission and hence cannot be a part of a traditional universal-jet model. In the uniform, sharp-edged jet picture the opening angles of the two outflow components are not invariant from source to source although their values may well be correlated. It is, however, conceivable that each of the two components is structured and that the jet is "universal" in the sense that this structure varies little from source to source. The basic implications of a structured two-component jet model would be similar to the ones that we discuss in § 3 in the context of a sharp-edged, uniform outflow, although some of the details may be different and would depend on the specifics of the angular distribution of E and η in each component (see, e.g., Kumar & Granot 2003 and B. Zhang et al. 2004).

In our simple treatment the interaction between the two jet components is neglected. This assumption can be justified even after the narrow component's jet-break time (see eq. [5] below), when the effects of sideways expansion could in principle become relevant (e.g., Rhoads 1999), in view of indications from recent numerical simulations (e.g., Kumar & Granot 2003; Cannizzo et al. 2004) that in practice there is relatively little lateral spreading so long as the jet is at least moderately relativistic. To further simplify the discussion we only consider the case of a uniform external medium (of number density $n = n_0\,\mathrm{cm}^{-3}$) and we neglect the possible effects of radiative losses on the hydrodynamic evolution (which may affect the early afterglow during the period of fast cooling if the fraction ϵ_e of the internal energy in electrons behind the afterglow shock is not $\ll 1$). The narrow and fast jet component has an initial Lorentz factor η_n ($\gtrsim 10^2$), a half-opening angle $\theta_{j,n}$, and a kinetic energy (at the beginning of the afterglow phase) E_n, while the wide and slow jet component is characterized by η_w (~ 10), $\theta_{j,w}$ ($> \theta_{j,n}$), and E_w. In the following, the subscripts 'n' and 'w' will denote the narrow and wide jet components, respectively. The ratio of the true energy E and the isotropic-equivalent energy E_{iso} is given by the beaming factor $f_b = 1 - \cos\theta_j \approx \theta_j^2/2$. Thus, $E_{iso,w}/E_{iso,n} = (\theta_{j,n}/\theta_{j,w})^2 E_w/E_n$.

The emission from each outflow component is calculated separately. For the early afterglow (while the reverse shock is still present) we use the results of Sari & Piran (1999a,b). For the emission during the subsequent self-similar evolution (Blandford & McKee 1976) we follow Sari et al. (1998), and for the post–jet-break emission we use the results of Sari et al. (1999). The typical synchrotron frequency ν_m, the cooling frequency ν_c, and the peak flux $F_{\nu,\max}$, of the emission from the shocked external medium behind the forward shock are

---

[3] In the simplified model used by Vlahakis et al. (2003), the value of $\theta_{j,w}$ could not be calculated exactly; in this paper we assume that it can be as large as $\sim 3\,\theta_{j,n}$.

given by

$$\nu_{\mathrm{m}} = 1.1 \times 10^{19} \, g^2 \epsilon_{\mathrm{e},-1}^2 \epsilon_{\mathrm{B},-1}^{1/2} n_0^{1/2} (\gamma/300)^4 \; \mathrm{Hz} \; , \quad (1)$$

$$\nu_{\mathrm{c}} = 1.1 \times 10^{17} \, \epsilon_{\mathrm{B},-1}^{-3/2} n_0^{-3/2} t_{\mathrm{s}}^{-2} (\gamma/300)^{-4} \; \mathrm{Hz} \; , \quad (2)$$

$$F_{\nu,\max} = 220 \, \epsilon_{\mathrm{B},-1}^{1/2} n_0^{3/2} D_{\mathrm{L},28}^{-2} t_{\mathrm{s}}^3 (\gamma/300)^8 \; \mu\mathrm{Jy} \quad (3)$$

(Sari & Piran 1999b), where $g \equiv 3(p-2)/(p-1)$, p is the power-law index of electron energy distribution $(dN_e/d\gamma_e \propto \gamma_e^{-p})$, $t = t_{\mathrm{s}}$ sec is the observed time, γ is the Lorentz factor of the shocked fluid, ϵ_B is the fraction of the internal energy behind the shock in the magnetic field, D_{L} is the the luminosity distance, and $Q_i \equiv Q/(10^i$ times the c.g.s. units of Q).

The interaction of the jet with the ambient medium initially drives a reverse shock into the GRB ejecta, which decelerates the ejecta. When the reverse shock is Newtonian, or at most mildly relativistic, then $\gamma \approx \eta$ over its entire duration and the energy given to the swept-up external medium (of rest mass M) is $\gamma^2 M c^2 \sim \eta^2 M c^2$. As this energy approaches E, the original kinetic energy of the ejecta, after

$$t_{\mathrm{dec}} = \frac{R_{\mathrm{dec}}}{2c\eta^2} = 0.49 \left(\frac{E_{\mathrm{iso},52}}{n_0}\right)^{1/3} \left(\frac{\eta}{10}\right)^{-8/3} \; \mathrm{days} \; , \quad (4)$$

significant deceleration must occur. For $t > t_{\mathrm{dec}}$ most of the energy is in the shocked external medium and a self-similar evolution is established (Blandford & McKee 1976). Since η_{w} is assumed to be rather small (~ 10), $t_{\mathrm{dec,w}}$ (~ 0.5 days) is much larger than the duration of the GRB. Therefore, the ejecta is always in the "thin shell" regime (Sari & Piran 1995; Sari 1997). In this case the reverse shock is initially Newtonian. It is natural to expect some variation in the initial Lorentz factor, $\Delta\eta \sim \eta$. For a thin shell, this causes the ejecta shell to start spreading long before the reverse shock finishes crossing the shell, which in turn causes the reverse shock to become mildly relativistic before the crossing has ended. In this paper we concentrate on the optical emission from the forward shock, which in the case of the fast component would dominate the optical flux from the reverse shock after $\sim 10^3$ sec for typical parameters (Kobayashi & Zhang 2003). In the case of the slow component, the contribution from the forward shock should typically dominate the optical flux at all times, with the emission from the reverse shock making a significant contribution only in the radio band (e.g., Piran et al. 2004).

When γ drops to $\sim \theta_{\mathrm{j}}^{-1}$ the edge of the jet becomes visible and sideways expansion may become noticeable. These two effects cause a break in the lightcurve at

$$t_{\mathrm{jet}} = 0.25 \, E_{\mathrm{iso},52}^{1/3} n_0^{-1/3} \theta_{j,-1}^{8/3} \; \mathrm{days} \; , \quad (5)$$

with the former effect evidently responsible for most of the steepening if the Lorentz factor is not too close to 1. Expressed in terms of the true energy, the jet-break time is

$$t_{\mathrm{jet}} = 0.66 \, E_{51}^{1/3} n_0^{-1/3} \theta_{j,-1}^2 \; \mathrm{days} \; . \quad (6)$$

In the early afterglow, at $t < t_{\mathrm{dec}}$, $\gamma \approx \eta$ (Sari & Piran 1999a,b). At $t_{\mathrm{dec}} < t \leq t_{\mathrm{jet}}$, $\gamma \sim \theta_{\mathrm{j}}^{-1}(t/t_{\mathrm{jet}})^{-3/8}$ (Sari et al. 1998). At $t > t_{\mathrm{jet}}$ (and before the nonrelativistic transition time t_{NR}), we have $\gamma \sim \theta_{\mathrm{j}}^{-1}(t/t_{\mathrm{jet}})^{-1/2}$

assuming rapid lateral expansion (Sari et al. 1999). Therefore, the temporal scalings of the break frequencies and peak flux are given by

$$\nu_{\mathrm{m}} \propto \gamma^4 \propto \begin{cases} t^0, & t < t_{\mathrm{dec}} \; , \\ t^{-3/2}, & t_{\mathrm{dec}} < t < t_{\mathrm{jet}} \; , \\ t^{-2}, & t > t_{\mathrm{jet}} \; , \end{cases} \quad (7)$$

$$\nu_{\mathrm{c}} \propto \gamma^{-4} t^{-2} \propto \begin{cases} t^{-2}, & t < t_{\mathrm{dec}} \; , \\ t^{-1/2}, & t_{\mathrm{dec}} < t < t_{\mathrm{jet}} \; , \\ t^0 & t > t_{\mathrm{jet}} \; , \end{cases} \quad (8)$$

$$F_{\nu,\max} \propto \gamma^8 t^3 \propto \begin{cases} t^3, & t < t_{\mathrm{dec}} \; , \\ t^0, & t_{\mathrm{dec}} < t < t_{\mathrm{jet}} \; , \\ t^{-1}, & t > t_{\mathrm{jet}} \; . \end{cases} \quad (9)$$

In the limit of negligible sideways expansion after the jet-break time, the time dependence of γ does not change at t_{jet}, so the behavior described by the second line in equations (7) and (8) continues to hold also for $t > t_{\mathrm{jet}}$. However, the maximum flux in this case is still reduced by a factor $(\theta_{\mathrm{j}}\gamma)^2$ (representing the ratio of the jet area to the beaming cone area) as t increases above t_{jet}, so t^{-1} in the last line of equation (9) is replaced by $t^{-3/4}$. For practical applications the qualitative behavior of the lightcurve in this limit is very similar to that in the limit of rapid lateral expansion, and since the expressions given in equations (7)–(9) are the ones commonly used in the literature, we continue to employ them in this work.

The transition time t_0 from fast cooling to slow cooling (when $\nu_m = \nu_c$), and the times t_m and t_c when ν_m and ν_c, respectively, pass by the observed frequency ν, are given by (Sari et al. 1998)

$$t_0 = 0.55 \, g^2 E_{\mathrm{iso},52} \epsilon_{\mathrm{e},-1}^2 \epsilon_{\mathrm{B},-1}^2 n_0 \; \mathrm{hr} \; , \quad (10)$$

$$t_{\mathrm{m}} = 0.36 \, g^{4/3} E_{\mathrm{iso},52}^{1/3} \nu_{15}^{-2/3} \epsilon_{\mathrm{e},-1}^{4/3} \epsilon_{\mathrm{B},-1}^{1/3} \; \mathrm{hr} \; , \quad (11)$$

$$t_{\mathrm{c}} = 0.17 \, E_{\mathrm{iso},52}^{-1} \nu_{15}^{-2} \epsilon_{\mathrm{B},-1}^{-3} n_0^{-2} \; \mathrm{hr} \; . \quad (12)$$

The transition frequency, ν_0, defined by $\nu_{\mathrm{m}}(t_0) = \nu_{\mathrm{c}}(t_0)$, is given by

$$\nu_0 = 5.5 \times 10^{14} g^{-1} E_{\mathrm{iso},52}^{-1} \epsilon_{\mathrm{e},-1}^{-1} \epsilon_{\mathrm{B},-1}^{-5/2} n_0^{-3/2} \; \mathrm{Hz} \; . \quad (13)$$

These transition times together with t_{dec} and t_{jet} separate the time domain into several segments. At each time segment, the flux is derived by comparing the observed frequency to ν_{m} and ν_{c} to determine the appropriate spectral behavior; one also makes sure to use the correct dynamical behavior for the given time segment. The explicit expressions for the flux contributions of the two outflow components at the different time segments are presented in Appendix A.

The ratio of the deceleration times of the two jet components is

$$\frac{t_{\mathrm{dec,w}}}{t_{\mathrm{dec,n}}} = \left(\frac{E_{\mathrm{iso,w}}}{E_{\mathrm{iso,n}}}\right)^{1/3} \left(\frac{\eta_{\mathrm{w}}}{\eta_{\mathrm{n}}}\right)^{-8/3} \; , \quad (14)$$

which for $\eta_n/\eta_w \sim 10$ is $\sim 10^3$. The deceleration time of the slow component is much larger than that of the fast component, so a bump would show up in the decaying lightcurve of the fast component due to the emission of the slow component if $F_{\nu,\mathrm{w}} > F_{\nu,\mathrm{n}}$ at $t = t_{\mathrm{dec,w}}$.

The flux ratio $(F_{\nu,\mathrm{w}}/F_{\nu,\mathrm{n}})_{t=t_{\mathrm{dec,w}}}$ depends on whether the slow/wide component decelerates before the jet-break time of the fast/narrow component or not (i.e.,

on the relative ordering of $t_{\rm dec,w}$ and $t_{\rm jet,n}$), since γ has different time evolution indices before and after jet break. From equations (4) and (5), the ratio of these two times is given by

$$\frac{t_{\rm dec,w}}{t_{\rm jet,n}} \approx A_1 \left(\frac{E_{\rm iso,w}}{E_{\rm iso,n}}\right)^{1/3} (\eta_{\rm w}\theta_{\rm j,n})^{-8/3} , \qquad (15)$$

where $A_1 = A_2 C_{\rm jet}^{8/3}$ and $A_2 \equiv C_t(t > t_{\rm dec})/C_t(t_{\rm dec}) \sim 1$ (with the coefficients $C_{\rm jet}$ and C_t defined from $\gamma(t_{\rm jet}) = C_{\rm jet}/\theta_{\rm j}$ and $t = R/C_t\gamma^2 c$). In this work we assume $C_{\rm jet} = 1$, $C_t(t_{\rm dec}) = 2$, and $C_t(t > t_{\rm dec}) = 4$, for which $A_1 = A_2 = 2$. However, in the figures of this paper we calculate the flux by using $C_t = 4$ at all times to ensure continuity of the plotted lightcurves; our algebraic expressions for the component flux ratios may therefore yield values that differ somewhat (by a factor $\lesssim 2$) from those implied by the presented figures.

From equations (3), (4), and the scaling of γ with time, the peak-flux ratio of the two components at $t_{\rm dec,w}$ is

$$\left.\frac{F_{\nu,\max,w}}{F_{\nu,\max,n}}\right|_{t=t_{\rm dec,w}} = \begin{cases} \frac{E_{\rm iso,w}}{E_{\rm iso,n}} & t_{\rm dec,w} < t_{\rm jet,n} \\ \left(\frac{E_{\rm iso,w}}{E_{\rm iso,n}}\right)\left(\frac{t_{\rm dec,w}}{t_{\rm jet,n}}\right) & t_{\rm dec,w} > t_{\rm jet,n} \end{cases} \quad (16)$$

The flux ratio under consideration also depends on the frequency range within which the observed frequency ν is located at $t_{\rm dec,w}$ for each of the two outflow components. For typical parameter values, $t_{\rm dec,w} > t_{\rm 0,n}$, so the narrow/fast component is in the slow cooling regime, $\nu_{\rm c,n}(t_{\rm dec,w}) > \nu_{\rm m,n}(t_{\rm dec,w})$. We also expect the wide/slow component to be slowly cooling (see eq. [A5]).

Based on the discussion in Appendix A, the R-band observation frequency $\nu_{\rm R} = 5 \times 10^{14}$ Hz exceeds both $\nu_{\rm m,w}(t_{\rm dec,w})$ and $\nu_{\rm m,w}(t_{\rm dec,n})$ for typical parameter values. However, $\nu_{\rm R}$ can be either larger or smaller than $\nu_{\rm c}$ for both components. There are thus four relevant cases: If $\nu_{\rm m}(t_{\rm dec,w}) < \nu < \nu_{\rm c}(t_{\rm dec,w})$ for both components, then

$$\left.\frac{F_{\nu,w}}{F_{\nu,n}}\right|_{t=t_{\rm dec,w}} = \frac{F_{\nu,\max,w}}{F_{\nu,\max,n}} \left(\frac{\nu_{\rm m,w}}{\nu_{\rm m,n}}\right)^{(p-1)/2} \equiv f_1$$

$$= \begin{cases} A_2^{3(p-1)/4} \left(\frac{E_{\rm iso,w}}{E_{\rm iso,n}}\right)^{(p+3)/4} \\ \qquad\qquad\qquad\qquad t_{\rm dec,w} < t_{\rm jet,n} , \\ A_1^{(p+3)/4} A_2^{3(p-1)/4} \left(\frac{E_{\rm iso,w}}{E_{\rm iso,n}}\right)^{(p+3)/3} \\ \quad \times (\eta_w\theta_{\rm j,n})^{-2(p+3)/3} \quad t_{\rm dec,w} > t_{\rm jet,n} . \end{cases} \quad (17)$$

This parameter regime applies to all the numerical examples presented in § 3. If $\nu > \nu_{\rm c}(t_{\rm dec,w}) > \nu_{\rm m}(t_{\rm dec,w})$ for both components, then

$$\left.\frac{F_{\nu,w}}{F_{\nu,n}}\right|_{t=t_{\rm dec,w}} = \frac{F_{\nu,\max,w}}{F_{\nu,\max,n}} \left(\frac{\nu_{\rm c,w}}{\nu_{\rm c,n}}\right)^{1/2} \left(\frac{\nu_{\rm m,w}}{\nu_{\rm m,n}}\right)^{(p-1)/2} \equiv f_2$$

$$= \begin{cases} A_2^{3(p-2)/4} \left(\frac{E_{\rm iso,w}}{E_{\rm iso,n}}\right)^{(p+2)/4} \\ \qquad\qquad\qquad\qquad t_{\rm dec,w} < t_{\rm jet,n} , \\ A_1^{(p+2)/4} A_2^{3(p-2)/4} \left(\frac{E_{\rm iso,w}}{E_{\rm iso,n}}\right)^{(p+2)/3} \\ \quad \times (\eta_w\theta_{\rm j,n})^{-2(p+2)/3} \quad t_{\rm dec,w} > t_{\rm jet,n} . \end{cases} \quad (18)$$

If $\nu > \nu_{\rm c,n}(t_{\rm dec,w})$, $\nu_{\rm m,w}(t_{\rm dec,w}) < \nu < \nu_{\rm c,w}(t_{\rm dec,w})$, then

$$\left.\frac{F_{\nu,w}}{F_{\nu,n}}\right|_{t=t_{\rm dec,w}} = f_1 \left(\frac{\nu}{\nu_{\rm c,n}}\right)^{1/2} = f_2 \left(\frac{\nu}{\nu_{\rm c,w}}\right)^{1/2} . \quad (19)$$

If $\nu_{\rm m,n}(t_{\rm dec,w}) < \nu < \nu_{\rm c,n}(t_{\rm dec,w})$, $\nu > \nu_{\rm c,w}(t_{\rm dec,w})$, then

$$\left.\frac{F_{\nu,w}}{F_{\nu,n}}\right|_{t=t_{\rm dec,w}} = f_1 \left(\frac{\nu}{\nu_{\rm c,w}}\right)^{-1/2} = f_2 \left(\frac{\nu}{\nu_{\rm c,n}}\right)^{-1/2} . \quad (20)$$

We find that, at $t_{\rm jet,w}$, $\nu_{\rm R} > \nu_{\rm m}$ and $\nu_{\rm c} > \nu_{\rm m}$ for both components over most of the characteristic parameter ranges (see Appendix A). Given also that the flux evolution after the jet break is the same for both components, it follows that the flux ratio after the two components have undergone a jet break is the same as that at $t_{\rm jet,w}$. From equations (3), (5), and (9), the peak-flux ratio of the two components at $t \geq t_{\rm jet,w}$ is [4]

$$\left.\frac{F_{\nu,\max,w}}{F_{\nu,\max,n}}\right|_{t \geq t_{\rm jet,w}} = \left(\frac{E_{\rm iso,w}}{E_{\rm iso,n}}\right)\left(\frac{t_{\rm jet,w}}{t_{\rm jet,n}}\right) = \left(\frac{E_{\rm w}}{E_{\rm n}}\right)^{4/3} . \quad (21)$$

Therefore (specializing to the case $t_{\rm dec,w} > t_{\rm jet,n}$), the flux ratio at $t_{\rm jet,w}$ assumes the same form as the flux ratio at $t_{\rm dec,w}$ after $\eta_{\rm w}$ is replaced by $1/\theta_{\rm jet,w}$ and all the characteristic frequencies are evaluated at $t_{\rm jet,w}$. Denoting by $\tilde{f}_i$ the same flux ratios as f_i for $i = 1, 2$, but evaluated at $t_{\rm jet,w}$ instead of at $t_{\rm dec,w}$, we obtain the following simple results:

$$\tilde{f}_1 \equiv \left.\frac{F_{\nu,w}}{F_{\nu,n}}\right|_{t=t_{\rm jet,w}}^{\nu < \nu_{\rm c}} = \left(\frac{E_{\rm w}}{E_{\rm n}}\right)^{(p+3)/3} \quad (22)$$

and

$$\tilde{f}_2 \equiv \left.\frac{F_{\nu,w}}{F_{\nu,n}}\right|_{t=t_{\rm jet,w}}^{\nu > \nu_{\rm c}} = \left(\frac{E_{\rm w}}{E_{\rm n}}\right)^{(p+2)/3} . \quad (23)$$

Another interesting quantity is the ratio of the fluxes from the two outflow components at the corresponding jet-break times, $\hat{f} \equiv F_{\nu,w}(t_{\rm jet,w})/F_{\nu,n}(t_{\rm jet,n})$. We find

$$\hat{f}_1 \equiv \left.\frac{F_{\nu,w}(t_{\rm jet,w})}{F_{\nu,n}(t_{\rm jet,n})}\right|_{\nu < \nu_{\rm c}} = \left(\frac{E_{\rm w}}{E_{\rm n}}\right)\left(\frac{\theta_{\rm j,w}}{\theta_{\rm j,n}}\right)^{-2p} \quad (24)$$

and

$$\hat{f}_2 \equiv \left.\frac{F_{\nu,w}(t_{\rm jet,w})}{F_{\nu,n}(t_{\rm jet,n})}\right|_{\nu > \nu_{\rm c}} = \left(\frac{E_{\rm w}}{E_{\rm n}}\right)^{2/3}\left(\frac{\theta_{\rm j,w}}{\theta_{\rm j,n}}\right)^{-2p} . \quad (25)$$

So far the calculations correspond to on-axis observers, i.e., $\theta_{\rm obs} = 0$. The results, however, apply to the entire range of observation angles $\theta_{\rm obs} \lesssim 1.5\,\theta_{\rm j}$, as demonstrated with the help of more realistic jet models (Granot et al. 2002). For off-axis observers with viewing angle $\theta_{\rm obs} \gtrsim 1.5\,\theta_{\rm j}$ the afterglow emission peaks at t_θ, the time when $\gamma \simeq \theta_{\rm obs}^{-1}$:

$$t_\theta = B \left(\frac{\theta_{\rm obs}}{\theta_{\rm j}}\right)^2 t_{\rm jet} \quad (26)$$

---

[4] In the simple jet model that we use (Rhoads 1999; Sari et al. 1999), the jet dynamics becomes independent of its initial opening angle at $t > t_{\rm jet}$ (Granot et al. 2002). Therefore, the lightcurves at any given viewing angle $\theta_{\rm obs}$ depend only on the true energy E of the outflow (in addition to the ambient density and microphysical parameters ϵ_e and ϵ_B, which are assumed to be the same for the two jet components). Thus, the flux ratios at a given observed time and frequency after both jet breaks (and both deceleration times) depend only on the ratio of their true energies, $E_{\rm w}/E_{\rm n}$.

(Nakar et al. 2002), where the model-dependent factor B is of the order of unity (we adopt $B = 1$ for the numerical estimates in this work). The lightcurve for $t > t_\theta$ is similar to the on-axis lightcurve. The maximum flux at t_θ strongly decreases with increasing viewing angle, as $F_{\max,\nu}(\theta_{\rm obs}) \propto \theta_{\rm obs}^{-2p}$ (see eqs. [9] and [10] of Nakar et al. 2002). As we discuss below, for $1.5\,\theta_{\rm j,n} \lesssim \theta_{\rm obs} \lesssim 1.5\,\theta_{\rm j,w}$ it is possible for the wide component to be visible first and for the narrow component to become dominant (at least temporarily) later. The estimate of equation (15) is now replaced by

$$\frac{t_{\rm dec,w}}{t_{\theta,n}} = \frac{A_1}{B}\left(\frac{E_{\rm w}}{E_{\rm n}}\right)^{1/3}(\frac{\theta_{\rm j,w}}{\theta_{\rm obs}})^2(\theta_{\rm j,w}\eta_{\rm w})^{-8/3} \ . \quad (27)$$

The emission from the wide and the narrow outflow components peaks at $t_{\rm dec,w}$ and $t_{\theta,n}$, respectively. In evaluating the effect of these peaks on the overall lightcurve, it is useful to consider two flux ratios: the quotient f^a of the first and second peak components, given by $F_{\nu,w}(t_{\rm dec,w})/F_{\nu,n}(t_{\theta,n})$ if $t_{\theta,n} > t_{\rm dec,w}$ and by its inverse if $t_{\theta,n} < t_{\rm dec,w}$, and the ratio f^b of the primary and secondary flux contributions at the time $t = \max\{t_{\rm dec,w}, t_{\theta,n}\}$ of the second peak. The ratio f^a determines which component dominates the overall lightcurve, whereas f^b indicates whether the secondary component can play a role in the late afterglow. As is the case at $t_{\rm jet,w}$, typically the R-band observation frequency at $t_{\theta,n}$ exceeds $\nu_{\rm m}$ and $\nu_{\rm c} > \nu_{\rm m}$ for both outflow components.

If $t_{\rm dec,w} > t_{\theta,n}$ then f^b (which in this case is the flux ratio of the wide component to the narrow component at $t_{\rm dec,w}$) is the same as the ratio f obtained in the on-axis case for $t_{\rm dec,w} > t_{\rm jet,n}$. The difference from the on-axis case is that the flux of the narrow component peaks at a later time ($t_{\theta,n}$) and is smaller. In this case

$$f^a = f^b \left(\frac{t_{\theta,n}}{t_{\rm dec,w}}\right)^p \quad (28)$$

or, written down explicitly,

$$f_1^a = B^p \left(\frac{A_2}{A_1}\right)^{3(p-1)/4} \left(\frac{E_{\rm w}}{E_{\rm n}}\right) \left(\frac{\theta_{\rm j,w}}{\theta_{\rm obs}}\right)^{-2p}$$
$$\times (\theta_{\rm j,w}\eta_{\rm w})^{2(p-1)} \ , \quad (29)$$

$$f_2^a = B^p \left(\frac{A_2}{A_1}\right)^{3(p-2)/4} \left(\frac{E_{\rm w}}{E_{\rm n}}\right)^{2/3} \left(\frac{\theta_{\rm j,w}}{\theta_{\rm obs}}\right)^{-2p}$$
$$\times (\theta_{\rm j,w}\eta_{\rm w})^{2(3p-2)/3} \ , \quad (30)$$

for the cases where $\nu < \nu_{\rm c}$ and $\nu > \nu_{\rm c}$, respectively. In order for a bump associated with the wide component to become visible during the late afterglow it is necessary for f^b to exceed 1. This condition requires $E_{\rm w}/E_{\rm n} > A_1^{-3/4}A_2^{-9(p-2)/4(p+2)}(\eta_w\theta_{\rm j,w})^2$ (see eqs. [17] and [18]). If f^a is also > 1 then the wide component dominates the entire lightcurve, with the narrow component possibly becoming visible as a bump on the curve's rising branch. If, however, both f^a and f^b are < 1 then the narrow component would dominate at all times.

When $t_{\rm dec,w} < t_{\theta,n} < t_{\rm jet,w}$, f^b is given by

$$f_1^b \equiv \left.\frac{F_{\nu,n}}{F_{\nu,w}}\right|_{t=t_{\theta,n}}^{\nu < \nu_{\rm c}}$$
$$= B^{-(p+3)/4}\left(\frac{E_{\rm n}}{E_{\rm w}}\right)^{(p+3)/4}\left(\frac{\theta_{\rm j,w}}{\theta_{\rm obs}}\right)^{(p+3)/2} \ , \quad (31)$$

$$f_2^b \equiv \left.\frac{F_{\nu,n}}{F_{\nu,w}}\right|_{t=t_{\theta,n}}^{\nu > \nu_{\rm c}}$$
$$= B^{-(p+2)/4}\left(\frac{E_{\rm n}}{E_{\rm w}}\right)^{(p+2)/4}\left(\frac{\theta_{\rm j,w}}{\theta_{\rm obs}}\right)^{(p+2)/2} \ , \quad (32)$$

whereas f^a is given by the inverse of the expression (eq. [28]) for $t_{\rm dec,w} > t_{\theta,n}$. In this case the condition $f^b > 1$, which requires $E_{\rm n}/E_{\rm w} > B(\theta_{\rm obs}/\theta_{\rm j,w})^2$ (see eqs. [31] and [32]), corresponds to the narrow component dominating the late afterglow. If also $f^a > 1$, then the narrow component dominates the entire lightcurve, with the wide component possibly becoming visible as a bump during the curve's initial rise. Conversely, when both f^a and f^b are < 1, then only the wide component's afterglow emission would be visible.

If the observer is located outside the solid angle subtended by the wide outflow component (i.e., $\theta_{\rm obs} \gtrsim 1.5\,\theta_{\rm j,w}$), then the flux contributions from the wide and the narrow components peak at $t_{\theta,w}$ and $t_{\theta,n}$, respectively. The ratio of these times is $t_{\theta,w}/t_{\theta,n} = (E_{\rm w}/E_{\rm n})^{1/3}$, which is independent of $\theta_{\rm obs}$. Thus, when $E_{\rm w} > E_{\rm n}$ then $t_{\theta,w} > t_{\theta,n}$, $f_1^a = E_{\rm w}/E_{\rm n}$, $f_2^a = (E_{\rm w}/E_{\rm n})^{2/3}$, and $f^b = \tilde{f}$. However, if $E_{\rm w} < E_{\rm n}$ then $t_{\theta,w} < t_{\theta,n}$, $f_1^a = E_{\rm n}/E_{\rm w}$, $f_2^a = (E_{\rm n}/E_{\rm w})^{2/3}$, and $f^b = \tilde{f}^{-1}$. All of these cases have $f^a > 1$ and $f^b > 1$, which means that the more energetic outflow component dominates the lightcurve for $t > \max\{t_{\theta,w}, t_{\theta,n}\}$.

3. APPLICATIONS

Our results have potentially significant implications to the interpretation of GRBs and XRFs. We consider these two applications separately, although our discussion makes it clear that they could be related under a unified picture of these sources.

3.1. *GRB Afterglows and Source Energetics*

We choose as fiducial parameters $\eta_{\rm n} = 200$, $\eta_{\rm w} = 15$, $\theta_{\rm j,n} = 0.05$ rad, $\theta_{\rm j,w}/\theta_{\rm j,n} = 3$, and $p = 2.2$. For this choice the ratio $t_{\rm dec,w}/t_{\rm jet,n}$ of the deceleration time of the wide component to the jet-break time of the narrow component (eq. [15]) ranges between 3.0 and 1.4 as $E_{\rm w}/E_{\rm n}$ decreases from 3 to 1/3. The near-coincidence of these two time scales can have interesting observational ramifications. In particular, if the flux ratio $(F_{\nu,w}/F_{\nu,n})_{t=t_{\rm dec,w}}$ is close to 1, then the presence of a break in the narrow component at $t_{\rm jet,n}$ may be masked by the rise in the flux from the wide component that occurs as $t_{\rm dec,w}$ is approached. For the adopted parameters, one finds from equations (17)–(20) that, in fact, $(F_{\nu,w}/F_{\nu,n})_{t=t_{\rm dec,w}} \gtrsim 1$ so long as $E_{\rm w}/E_{\rm n}$ is $\gtrsim 2$, but that the flux ratio becomes $\ll 1$ for low values of the wide-to-narrow injected energy ratio. For example, in the case described by equation (17), $(F_{\nu,w}/F_{\nu,n})_{t=t_{\rm dec,w}} = 1.9$, 0.3, and 0.04 for $E_{\rm w}/E_{\rm n} = 3$, 1, and 1/3, respectively. For $t > t_{\rm dec,w} > t_{\rm jet,n}$ the flux from the wide component decreases with time no faster than $t^{-(3p-2)/4}(= t^{-1.15})$ or even increases with t (for $t_{\rm dec,w} < t < \min\{t_{m,w}, t_{\rm jet,w}\}$; see eqs. [A6]–[A11]), whereas the flux from the narrow component decreases steeply (as t^{-p}; eqs. [A1]–[A4]). Thus, even if $F_{\nu,w}$ is still $< F_{\nu,n}$ at $t = t_{\rm dec,w}$ (i.e., $f_1 < 1$), when $E_{\rm w} > E_{\rm n}$
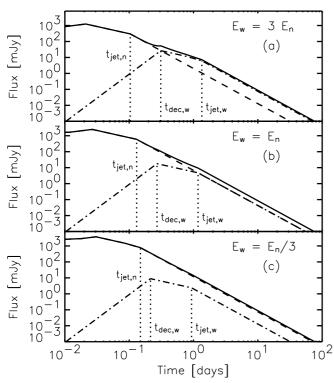
FIG. 1.— R-band afterglow lightcurve from a two-component jet. The contribution of the narrow component, wide component, and their sum is represented by the dashed, dash-dotted, and solid curves, respectively. The total outflow energy is assumed to be constant, $E_{\rm w} + E_{\rm n} = 10^{51}$ ergs. From top to bottom, the 3 panels correspond to $E_{\rm w}/E_{\rm n} = 3$, 1, and 1/3, respectively. The other parameters are the same for all panels: $\eta_{\rm n} = 200$, $\eta_{\rm w} = 15$, $\theta_{\rm j,w} = 0.15$, $\theta_{\rm j,n} = 0.05$, $n_0 = 1$, $\epsilon_e = 0.1$, $\epsilon_B = 0.01$, $p = 2.2$, and $D_{\rm L,28} = 1$.

it will become the dominant contributor to the total afterglow flux soon thereafter. (In the case described by eq. [17], this will occur for $t/t_{\rm dec,w} > f_1^{-4/(p+2)}$.) As illustrated by the model lightcurve plotted in Figure 1a, a clear signature of a jet break in the lightcurve would occur, under these circumstances, only at $t = t_{\rm jet,w}$.

The possibility that the jet break in the narrow outflow component remains unobservable could have important consequences for the inferred energetics of GRBs. Recall that it has been found (Frail et al. 2001; Bloom et al. 2003) that, when the isotropic-equivalent γ-ray energies of a sample of GRBs are converted into true energies by using the beaming factor inferred from the observed jet break, then the resulting values cluster narrowly about $E_\gamma \approx 10^{51}$ ergs. On the other hand, the isotropic-equivalent kinetic energies of GRB outflows, as estimated from dynamical and spectral modeling of the associated afterglows, yield — after being corrected by the jet break-inferred beaming factor — a narrow distribution of true kinetic energies (for 2 oppositely directed jets) at the beginning of the afterglow phase that is centered on $E \approx 10^{51}$ ergs (Panaitescu & Kumar 2002; see also Yost et al. 2003). A similar result is obtained when the afterglow X-ray luminosity is used as a surrogate for the isotropic-equivalent outflow kinetic energy (Berger et al. 2003a). The X-ray emission typically peaks during the early afterglow, so the kinetic energy estimated on the basis of the X-ray luminosity (and con-

ventionally evaluated at $t = 10$ hr) likely corresponds to that of the *narrow* outflow component. However, the X-ray–based isotropic-equivalent kinetic energy is typically found to be smaller than the isotropic-equivalent kinetic energy inferred from the spectral and dynamical modeling of the overall afterglow (which, for $E_{\rm w} > E_{\rm n}$, is dominated by the contribution of the wide component). In the context of the two-component jet model this implies that the wide component should dominate also at early times, which is clearly inconsistent. The X-ray–based isotropic-equivalent kinetic energy typically also turns out to be smaller than the isotropic-equivalent γ-ray energy, which in a two-component model that associates the γ-rays with the narrow core would be difficult to reconcile with the internal-shock scenario of GRBs (see discussion in the next paragraph). It is therefore quite possible that the X-ray–based deduction systematically underestimates the true kinetic energy in the narrow outflow component.

The approximate equality of the inferred values of E_γ and E has been given several different explanations; here we focus on its interpretation in the context of the internal-shock scenario for GRBs (Rees & Mészáros 1994), which has been successful at accounting for the observed variability properties of the bursts (e.g., Nakar & Piran 2002). In this picture, the γ-ray emission originates in shocks that form in the collisions of "shells" that are injected with variable energy and/or mass at the origin. It was shown (Beloborodov 2000; Kobayashi & Sari 2001) that E_γ/E can in principle be ~ 1 in this case if the following conditions are satisfied: (1) the spread between the minimum and maximum initial Lorentz factors of the shells is large enough ($\gamma_{\rm i,max}/\gamma_{\rm i,min} \lesssim 10$); (2) the distribution of initial Lorentz factors is sufficiently nonuniform (one possibility being that $\log \gamma_{\rm i}$, rather than $\gamma_{\rm i}$, is distributed uniformly); (3) the shells are approximately of equal mass and their number is large enough ($\gtrsim 30$), and (4) the fraction of the dissipated energy that is deposited in electrons and then radiated away is sufficiently high ($\epsilon_e \gtrsim 0.3$), with a similar constraint applying to the fraction of the radiated energy that is emitted as gamma-rays. If any of these conditions were violated to a significant extent then the implied magnitude of E_γ/E could decrease to a value well below 1.

We do not at present have independent information about the nature of GRB outflows to verify that the above conditions are indeed satisfied in the majority of sources, as would be required for consistency between the internal-shock model and the inferred distributions of E_γ and E. It is, however, worth noting that these constraints can in principle be alleviated if the outflows correspond to two-component jets with $E_{\rm w} \gtrsim E_{\rm n}$.[5] This is because the inference $E_\gamma/E \sim 1$ is based on the assumption that the solid angle used to convert the isotropic-equivalent energy into a true energy is the same for the γ-rays and the afterglow radiation. If $E_{\rm w} \gtrsim E_{\rm n}$ then most of the afterglow radiation will be emitted from the wide component and the value of E will be appropriately inferred from $E_{\rm iso}$ using the opening half-angle of the wide outflow component, $\theta_{\rm j,w}$. However, as the prompt

_____
[5] This possibility was originally noted in a talk at the 2003 GRB meeting in Santa Fe; see Königl (2004).

high-energy emission in this picture originates in the narrow outflow component, the conversion of the isotropic-equivalent γ-ray energy into E_γ must be done using the opening half-angle of the narrow component, $\theta_{j,n}$. If, as discussed above, the jet break in the narrow component is not observationally discernible and the outflow is mistakenly interpreted as a single-component jet with an opening half-angle $\theta_{j,w}$, then E_γ will be *overestimated* by a factor $\sim (\theta_{j,w}/\theta_{j,n})^2$ ($= 9$ for the fiducial values adopted in this paper). The actual magnitude of E_γ in this case could thus be well below the value inferred on the basis of a single-component jet model.

Kumar & Piran (2000b) proposed that the ejected material in GRB outflows exhibits strong angular fluctuations, forming "patchy" shells. In this case the conversion from an isotropic-equivalent to a true energy also involves a smaller effective solid angle for the γ-ray emission than for the afterglow radiation. This situation could in principle be distinguished from the two-component outflow scenario discussed in this paper through some of the specific predictions of each of these models. For example, Kumar & Piran (2000b) argue that a patchy-shell outflow could exhibit large temporal fluctuations (with a progressively decreasing amplitude) during the early (minutes to hours) afterglow, whereas the results derived in this paper indicate that the afterglow lightcurve produced by a two-component jet with $E_w \gtrsim E_n$ might temporarily depart from a simple power-law decay around $t \approx t_{dec,w}$ (over a timescale of hours).[6] It is, however, conceivable that the ejected shell may be patchy even if the outflow has more than one component.

As we have shown, the possibility that E_γ is overestimated in a two-component outflow can only be realized if E_w exceeds E_n. However, in order for the high-efficiency requirement on the emission from internal shocks (and the corresponding conditions listed above) to be relaxed, the ratio E_w/E_n cannot be much greater than 1. Specifically, the kinetic-to-radiative energy conversion efficiency of the narrow outflow component, $\mathcal{E}_n \equiv E_\gamma/(E_\gamma + E_n)$, is determined by the ratio E_γ/E_n, which is overestimated by the factor $(E_n/E_w)(\theta_{j,w}/\theta_{j,n})^2 = E_{iso,n}/E_{iso,w}$ if $E \approx E_w$.[7] Thus, to have any reduction in the required efficiency, $E_{iso,n}/E_{iso,w}$ must exceed 1. The above two constraints can be expressed as a double inequality on the ratio of the component kinetic energies:

$$1 < E_w/E_n < (\theta_{j,w}/\theta_{j,n})^2 . \tag{33}$$

The condition $E_w/E_n > 1$ implies that the wide component dominates the afterglow emission at late times (see eqs. [21]-[23]), whereas the requirement $E_{iso,n}/E_{iso,w} > 1$ implies that the narrow component dominates at early times (see eqs. [16]-[20]).

A two-component outflow with $E_w/E_n \gtrsim 1$ arises naturally in the (initially) neutron-rich, hydromagnetically accelerated jet scenario (see § 1). In contrast, in the two-component outflow investigated in the context of the collapsar model, the ratio E_w/E_n is typically $\ll 1$ and hence (see Fig. 1c) the optical after-
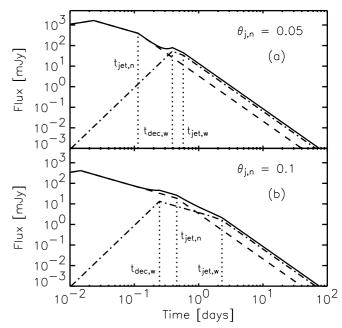
---

[6] As discussed below, refreshed shocks are another likely source of lightcurve variability (on timescales of hours to days).

[7] If the kinetic energy inferred from the afterglow fitting in fact corresponds to the sum of the contributions from the wide and narrow components, then the factor E_n/E_w in the overestimation expression is replaced by $1/(1 + E_w/E_n)$.

FIG. 2.— Similar to Fig. 1, except that $E_w = 2 E_n$ and $\theta_{j,w} = 2 \theta_{j,n}$. The top and bottom panels correspond to $\theta_{j,n} = 0.05$ and 0.1, respectively. The other parameters are the same as in Fig. 1.

glow emission from the wide (cocoon) component would generally remain undetectable at all times. For the adopted fiducial parameters and assuming $E_w/E_n = 0.1$, $t_{dec,w}/t_{jet,n} = 0.96$ and, for the case described by equation (17), $(F_{\nu,w}/F_{\nu,n})_{t=t_{dec,w}} = 5 \times 10^{-3}$. Note, however, that the cocoon afterglow emission might dominate at early times at submillimeter wavelengths and that there may also be a signature in the early optical afterglow of the collision between the expanding cocoon and the decelerating head of the narrow outflow component (Ramirez-Ruiz et al. 2002).

The plots in Figure 1 demonstrate that the optical afterglow lightcurve from a two-component jet departs from a simple power-law decay when the flux contributions from the two components become comparable, which for a jet with $E_w \gtrsim E_n$ typically occurs around the deceleration time of the wide component. As the wide component gradually takes over from the narrow component to become the dominant contributor to the flux, the lightcurve exhibits a concave "flattening" (if $t_{dec,w} > t_{jet,n}$; see Fig. 2a) or a convex "bump" (if $t_{dec,w} < t_{jet,n}$; see Fig. 2b) of duration $\Delta t \sim t$. The presence of this feature may be hard to discern in practice because of insufficiently dense time coverage or the interference of other factors (the emission from the reverse shock, ambient density inhomogeneities, refreshed shocks, etc.) that could cause a similar behavior. Nonetheless, there are already several potential candidates for this feature among observed afterglows. For example, GRB 970508 exhibited a pronounced brightening between ~ 1 and ~ 2 days, after which it followed an approximate power-law decay (e.g., Pedersen et al. 1998). However, between ~ 0.1 and ~ 1 day the lightcurve was constant or slightly declining with time, a behavior that is not reproduced by our simple two-component jet model.[8] A ma-

---

[8] In our picture, the brightening would be caused by a wide

jor brightening event was also recorded in GRB 021004 around ~ 0.1 days (e.g., Fox et al. 2003). In this case, the lightcurve assumed a flat form between ~ 0.02 and ~ 0.1 days and a power-law decay index of ~ 1.2 immediately thereafter (Uemura et al. 2003), which is consistent with the behavior expected in the two-component model (see Figs. 1a and 2a; if this brightening is indeed associated with the emergence of the wide-component emission then the inferred power-law index implies, by eq. [A6], $p \approx 2.2$ for this component). The identification of the brightening time with $t_{\rm dec,w}$ suggests that the wide component in this source had a comparatively high value of $\eta_{\rm w}$ (see eq. [4]).

An alternative interpretation of the early brightening in GRB 021004 was given by Kobayashi & Zhang (2003), who attributed it to the emission of the forward shock taking over from that of the reverse shock. It is, however, worth noting that GRB 021004 exhibited a second, less pronounced brightening at $t \approx 1$ day and possibly a third one at $t \approx 3$ days, and that it has been suggested that all these events may have a similar physical origin — either a variable external density (Lazzati et al. 2002) or energy fluctuations that, in turn, could arise either from variable injection at the source (refreshed shocks) or from a patchy angular structure of the outflow (Nakar et al. 2003). Interestingly, a refreshed-shock scenario is a natural feature of the hydromagnetic, initially neutron-rich jet model of Vlahakis et al. (2003). In this picture, the decoupled neutrons that constitute the wide outflow component decay into protons on a distance scale $\gtrsim R_\beta = 4 \times 10^{14}(\eta_{\rm w}/15)$ cm, which is likely larger than the scale over which many of the shell collisions invoked in the internal shock model for GRBs take place. Shell collisions may well give rise to the γ-ray emission from the narrow (proton) outflow component, but since they cannot take place inside the wide component before the neutrons are converted into protons, all the fast shells that overtake slower shells at $R \lesssim R_\beta$ would become arranged in a sequence wherein the faster shells are in the front and the slower ones lag behind and remain closer to the origin. Furthermore, the radius at which the neutron shells are arranged in this way is smaller by a factor of $\sim (\eta_{\rm n}/\eta_{\rm w})^2$ compared to the radius of the internal shocks, and is thus $\ll R_\beta$. The neutron shells can therefore pass through each other with very little interaction between them while ordering themselves according to their velocities. After the decay into protons the wide outflow component would start sweeping up the ambient mass, which would cause it to decelerate. Under these circumstances, the slower shells that had been left behind would overtake the decelerated front shell, leading to a pileup as progressively lower-η shells arrive at correspondingly later times. The wide-component afterglow would then assume the form of a repeatedly reenergized shock, with the energy injection occurring quasi-continuously at first and then possibly tapering off as the slowest shells finally arrive at the front-shock location. This picture is broadly compatible with the observations of GRB 021004: the large initial brightening may be in-

terpreted as the quasi-continuously energized early afterglow emission from the wide outflow component, and the subsequent rebrightenings may be attributed either to collisions with late-arriving shells (e.g., Kumar & Piran 2000a) or to a patchy angular structure (for which other aspects of the afterglow provide independent support; see Nakar & Piran 2003 and Nakar & Oren 2004).

Similarly to GRB 021004, GRB 030329 manifested a significant brightening in its optical lightcurve (at $t \approx 1.5$ days), followed by several less pronounced rebrightenings (at $t \approx 2.6$, 3.3, and 5.3 days, respectively). Granot et al. (2003) and Piran et al. (2004) argued that these brightening episodes can be interpreted in terms of refreshed shocks in a single-component jet that reenergize the afterglow emission after the jet-break time (at ~ 0.5 days). An alternative interpretation of the prominent initial brightening in terms of the emergence of the wide component in a two-component outflow was given by Berger et al. (2003b) and Sheth et al. (2003). They identified the early break in the optical lightcurve with $t_{\rm jet,n}$, the initial brightening with $t_{\rm dec,w}$, and a subsequent break in the radio lightcurve at ~ 10 days with $t_{\rm jet,w}$.[9] To apply our two-component model to this source, we adopt the latter interpretation and consider the early afterglow lightcurve ($t \lesssim 1$ day) as having been dominated by the narrow outflow component. We incorporate the apparent presence of refreshed shocks by taking the value of $E_{\rm w}$ at $t_{\rm jet,w}$ as being ~ 3 times larger than the corresponding value at $t_{\rm dec,w}$ (see Granot et al. 2003). We adopt $E_{\rm iso,w,52}/n_0 \approx 30$ at $t = t_{\rm jet,w}$ on the basis of the (rather uncertain) estimates obtained from fitting the sizes of the radio images of this afterglow at $t = 24$ and 83 days (Taylor et al. 2004; Granot et al. 2005). Using this value in equation (5) and $E_{\rm iso,w,52}/n_0 \approx 10$ in equation (4), we infer $\theta_{\rm j,w} = 0.26$ and $\eta_{\rm w} = 8.8$, respectively. Adopting $p = 2.25$ from the early-afterglow spectral fit of Willingale et al. (2004), we extend the narrow-component's flux from $t_{\rm jet,n}$ to $t_{\rm dec,w}$ and deduce $f_1 = F_{\nu,\rm w}(t_{\rm dec,w})/F_{\nu,\rm n}(t_{\rm dec,w}) \approx 2.3$. Equations (4), (5), and (17) then yield $E_{\rm iso,w}/E_{\rm iso,n} = 0.38$ and $\eta_{\rm w}\theta_{\rm j,n} = 0.76$. We thus infer $\theta_{\rm j,n} \approx 0.086$. As a check on these deductions, we calculate the flux ratio $\hat{f}_1 = F_{\nu,\rm w}(t_{\rm jet,w})/F_{\nu,\rm n}(t_{\rm jet,n})$ using equation (24). We obtain $\hat{f}_1 \approx 0.025$, which agrees well with the observed value of ~ 0.033 given that $\sim 20\%$ of the observed flux at $t_{\rm jet,w}$ appears to have come from the associated supernova SN 2003dh (Berger et al. 2003b; Lipkin et al. 2004). To estimate the true energy of the two outflow components, we assume that the measured isotropic-equivalent γ-ray energy of this burst ($\simeq 10^{52}$ ergs; Price et al. 2003, Hjorth et al. 2003) has been produced by the narrow component with a radiative efficiency ~ 0.2, which implies $E_{\rm iso,n,52} \approx 5$ and hence $n_0 \approx 0.19$. The latter value is consistent with the density estimates obtained from spectral modeling of the afterglow (e.g., Berger et al. 2003b; Willingale et al. 2004; Granot et al. 2005). In this way we deduce $E_{\rm w,50} \approx 6.4$ and $E_{\rm n,50} \approx 1.8$.

An illustrative two-component model lightcurve based on the above estimates is shown in Figure 3. The values of the parameters ϵ_e and ϵ_B in this fit were chosen

---

component with $E_{\rm w} \gtrsim E_{\rm n}$ that is observed at $\theta_{\rm obs} \lesssim \theta_{\rm j,n}$ and peaks at $t = t_{\rm dec,w}$. In contrast, Panaitescu et al. (1998) attributed the flux rise to a narrow jet seen outside its opening half-angle and suggested that the flux at earlier times could be produced by a wide (essentially isotropic) component of lower energy.

[9] A milder break around 0.25 days can be interpreted as corresponding to the transition time $t_{\rm c}$ (eq. [12]); see Lipkin et al. (2004).
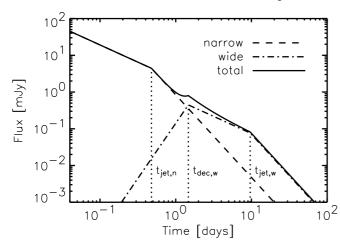
FIG. 3.— R-band lightcurve from a two-component model with parameters appropriate to GRB 030329 ($D_{\rm L} = 0.8$ Gpc): $\eta_{\rm n} = 200$, $\eta_{\rm w} = 8.8$, $E_{\rm w} = 6.4 \times 10^{50}$ ergs, $E_{\rm n} = 1.8 \times 10^{50}$ ergs, $\theta_{\rm j,w} = 0.26$, $\theta_{\rm j,n} = 0.086$, $n_0 = 0.19$ cm^{-3}, $\epsilon_e = 0.01$, $\epsilon_B = 0.008$, and $p = 2.25$.

somewhat arbitrarily to approximate the measured flux level (which is mostly sensitive to ϵ_e). The value of $\eta_{\rm n}$ cannot be inferred from the available observations and was simply chosen to be $\gg \eta_{\rm w}$. Although this simple model can account for the presence of the pronounced bump at $t \approx 1.5$ days, the model lightcurve (which in general cannot rise faster than $\propto t^3$; see eqs. [A6]–[A11]) cannot readily reproduce the sharpness of the observed flux increase at that time. The steep rise might, however, be explained by the refreshed-shock model (e.g., Granot et al. 2003). This possibility is consistent with observational evidence that the "shock refreshing" process in this source was already under way at $t = t_{\rm dec,w}$ (Willingale et al. 2004; Lipkin et al. 2004). As noted above in connection with GRB 021004, the occurrence of such shocks around $t_{\rm jet,w}$ can be naturally expected in the hydromagnetic, initially neutron-rich outflow scenario. It is worth pointing out, however, that other potential problems with the two-component interpretation of the GRB 030329 data still remain to be addressed. In particular (see Piran et al. 2004), the strong radio signature from a reverse shock that is expected in this picture at $t \approx t_{\rm d,w}$ has not been detected.

The afterglows of GRB 021004 and GRB 030329 were distinguished by the fact that their monitoring started early on and was conducted with particularly high time resolution and precision. Future observations will determine whether the departure from a smooth power-law behavior exhibited by the lightcurves from these two sources is a common feature of GRB afterglows. If this turns out to be the case, then the possibility that this behavior is associated with the decoupling of a neutron component in a hydromagnetically driven jet would merit a closer examination.

3.2. XRF Afterglows and Source Energetics

X-ray flash (XRF) sources (e.g., Heise 2003; Kippen et al. 2003) are high-energy transients that strongly resemble GRBs except that their peak energies fall in the X-ray, rather than the γ-ray, spectral regime. One attractive interpretation of these sources is that they represent essentially uniform GRB jets that are observed outside the jet half-opening angle, $\theta_{\rm obs} > \theta_{\rm j}$ (e.g., Yamazaki et al. 2002, 2004). In this picture, the larger viewing angle results in a smaller Doppler factor and hence a lower apparent peak frequency than in GRBs, which correspond to $\theta_{\rm obs} < \theta_{\rm j}$. The association with GRBs has received support from the detection of afterglow emission in several XRF sources. In particular, Soderberg et al. (2004) carried out the first spectroscopic observations of an XRF and form modeling of the radio afterglow of XRF 020903 inferred that its total kinetic energy is comparable to that typically deduced in GRB sources. The relatively low isotropic equivalent energy of the prompt-emission in XRF 020903, $E_{\rm X,iso} \approx 1.1 \times 10^{49}$ ergs, is ~ 2 orders of magnitude smaller than the narrowly clustered values for the true energy output in gamma-rays deduced for GRBs, $E_\gamma \approx 10^{51}$ ergs (Frail et al. 2001; Bloom et al. 2003), which is itself $\sim 1 - 3$ orders of magnitude smaller than the isotropic equivalent gamma-ray energy output in GRBs, $E_{\gamma,\rm iso} \sim 10^{52} - 10^{54}$ ergs. This is consistent with the expected reduction in the measured fluence for off-axis observers as a result of the decrease in the Doppler factor.[10]

In the context of a two-component outflow model with $E_{\rm w} \gtrsim E_{\rm n}$, the above unified GRB/XRF picture leads to the identification of XRFs with GRB outflows that are observed at $\theta_{\rm obs} > \theta_{\rm j,n}$ but likely still within the opening half-angle of the wide component. Using our fiducial model parameters and assuming $\theta_{\rm obs} = 2\,\theta_{\rm j,n}$, we find that $t_{\rm dec,w}/t_{\theta,\rm n} = 0.65$ and 0.75 (eq. [27]) and that $[F_{\nu,\rm n}/F_{\nu,\rm w}](t = t_{\theta,\rm n}) = 0.43$ and 0.28 (eq. [31]) for $E_{\rm w}/E_{\rm n} = 2$ and 3, respectively. Thus, even though the wide component would dominate the overall afterglow emission, the narrow component might give rise to a bump in the optical lightcurve around $t_{\theta,\rm n}$. In fact, a bump in the afterglow lightcurve of XRF 030723 was interpreted along these lines by Huang et al. (2004), who employed a two-component outflow model with $\theta_{\rm j,w} \approx 3\,\theta_{\rm j,n}$ and $E_{\rm n} \approx 3\,E_{\rm w}$. To account for the relatively late occurrence of this bump (between ~ 11 and ~ 14 days), a rather large observation angle was adopted in this fit ($\theta_{\rm obs} = 0.37\,{\rm rad} \approx 4\,\theta_{\rm j,n}$; see eq. [26]). However, the rebrightening of XRF 030723 was found to be accompanied by a significant spectral reddening (Fynbo et al. 2004), which is not naturally explained in the two-component model but could possibly be associated with a supernova. Further tests of this aspect of the two-component model would therefore need to await the detection of additional examples of bumps in XRF afterglow lightcurves by future observations.

An alternative interpretation of XRFs has been proposed in the context of the $E_{\rm n} > E_{\rm w}$ two-component collapsar outflow model (e.g., W. Zhang et al. 2004). In this picture, the transient X-ray emission is attributed to external shocks driven by the wide (cocoon) component. Although the detailed implications of this proposal have not yet been fully worked out, this scenario could conceivably account for the large inferred ratio of the transient radiation energy and the afterglow kinetic en-

---

[10] The fluence decreases as the third power of the Doppler factor (Granot et al. 2002), one power from the reduced energy of each photon and a power of two from the relativistic beaming of the photons (aberration of light) away from our line of sight.

ergy in XRF 020903 by associating the afterglow emission with the external shock of the more energetic narrow (jet-core) component. However, since the afterglow emission from the narrow component only becomes observable for $t > t_{\theta,\mathrm{n}}$, it should exhibit a rapid decline with time, which may not be consistent with the data from XRF 020903 (where Soderberg et al. 2004 still detected radio afterglow emission after ~ 200 days).

4. CONCLUSIONS

In this paper we study the optical afterglow lightcurves produced by GRB sources that have two distinct outflow components. The possibility that GRB jets have a narrow/fast core and a wider/slower outer component has been indicated by observations of both the γ-ray and the afterglow emission (including the afterglows of GRB 970508, GRB 991216, and GRB 030329) and independently by theoretical considerations. Since we are interested in the distinct afterglow signatures of the two components, we focus on models in which the Lorentz factors of both outflow components are initially $\gg 1$. We choose the hydromagnetically driven, initially neutron-rich jet model of Vlahakis et al. (2003) and the collapsar jet-breakout model of W. Zhang et al. (2004) as being representative of scenarios in which the dual nature of the outflow reflects initial conditions and propagation effects, respectively. In both of these models the characteristic initial Lorentz factor and opening half-angles are $\eta_{\mathrm{n}} \gtrsim 10^2$ and $\theta_{\mathrm{j,n}} \sim 0.05$ for the narrow component and $\eta_{\mathrm{w}} \sim 10$, $\theta_{\mathrm{j,w}} \lesssim 3\,\theta_{\mathrm{j,n}}$ for the wide one, and the γ-ray emission originates in the narrow component. They are distinguished, however, by the ratio of the kinetic energy injected into the two components: $E_{\mathrm{w}}/E_{\mathrm{n}} \sim 0.1$ for the collapsar model and $\gtrsim 2$ for the neutron-rich hydromagnetic model (with $E_{\mathrm{w}} + E_{\mathrm{n}}$ inferred to be $\sim 10^{51}$ ergs).

Using a simple synchrotron emission model, we calculate the afterglow emission produced by the shocks that the two components drive into the ambient medium. We derive useful algebraic expressions for the component flux ratios at the main transition times in the light curve (in particular, the wide component's deceleration time $t_{\mathrm{dec,w}}$ and the jet-break times $t_{\mathrm{jet,w}}$ and $t_{\mathrm{jet,n}}$) for the cases where the observation angle θ_{obs} satisfies $\theta_{\mathrm{obs}} < 1.5\,\theta_{\mathrm{j,n}}$ and $1.5\,\theta_{\mathrm{j,n}} < \theta_{\mathrm{obs}} < 1.5\,\theta_{\mathrm{j,w}}$, respectively (where in the latter case $t_{\theta,\mathrm{n}}$ is the relevant break time for the narrow component). We study the behavior of the optical lightcurves for different values of $E_{\mathrm{w}}/E_{\mathrm{n}}$ and find that, for the adopted characteristic parameters, the contribution of the narrow component dominates at all times if this ratio is $\ll 1$ (as in the collapsar jet-breakout model), but that the contribution of the wide component becomes dominant for $t \gtrsim t_{\mathrm{dec,w}}$ if $E_{\mathrm{w}} \gtrsim 2\,E_{\mathrm{n}}$ (as in the neutron-rich hydromagnetic model). The emergence of the wide component may be related to the pronounced brightening detected in the lightcurves of several afterglows $\sim 0.1 - 1$ days after the GRB (see Fig. 3).

For typical parameter values $t_{\mathrm{dec,w}}$ is found to be comparable to $t_{\mathrm{jet,n}}$. It follows that, if $E_{\mathrm{w}} > E_{\mathrm{n}}$, then

the steepening of the narrow component's lightcurve at $t \gtrsim t_{\mathrm{jet,n}}$ could be masked by the emergence (and subsequent dominance) of the wide component (see Fig. 1). Under these circumstances, the only clearly discernible jet break in the optical lightcurve would occur at $t_{\mathrm{jet,w}}$. We suggest that this may have led to an overestimate of the emitted γ-ray energy in many GRBs because the wide component's opening half-angle $\theta_{\mathrm{j,w}}$ — rather than the narrow component's angle $\theta_{\mathrm{j,n}}$ — was used in converting the measured $E_{\gamma,\mathrm{iso}}$ into the true energy E_{γ}. This, in turn, would have led to an overestimate [by a factor $\sim (E_{\mathrm{n}}/E_{\mathrm{w}})(\theta_{\mathrm{j,w}}/\theta_{\mathrm{j,n}})^2 = E_{\mathrm{iso,n}}/E_{\mathrm{iso,w}}$] of the ratio $E_{\gamma}/E_{\mathrm{n}}$ that determines the kinetic-to-radiative energy conversion efficiency of the outflow. Factoring in this overestimate [which can be done when the component kinetic energies satisfy $1 < E_{\mathrm{w}}/E_{\mathrm{n}} < (\theta_{\mathrm{j,w}}/\theta_{\mathrm{j,n}})^2$] would alleviate the need to account for conversion efficiencies $O(1)$ in internal shock models of GRBs. Dense monitoring of the afterglow lightcurve during the time interval ($\sim 0.1 - 1$ days) that encompasses $t_{\mathrm{jet,n}}$ and $t_{\mathrm{dec,w}}$ could provide a test of this suggestion. If $t_{\mathrm{jet,n}} \lesssim t_{\mathrm{dec,w}}$ then the lightcurve should exhibit a convex bump during this time interval, whereas if this inequality is reversed a concave flattening would be expected (see Fig. 2). The above considerations also apply to jets observed at $\theta_{\mathrm{obs}} \gtrsim 1.5\,\theta_{\mathrm{j,n}}$, which would be perceived as X-ray flash sources. For $E_{\mathrm{w}} > E_{\mathrm{n}}$, the afterglow emission from such sources would be dominated by the wide outflow component, although the narrow component might give rise to a bump in the lightcurve at $t \approx t_{\theta,\mathrm{n}}$.

The well-monitored afterglow lightcurves of GRB 021004 and GRB 030329 exhibited a significant early brightening that was followed by several less pronounced rebrightenings on a time scale of days. These episodes can be satisfactorily interpreted as refreshed shocks. We point out that the initially neutron-rich hydromagnetic jet model, in which the decoupled protons and neutrons give rise to a narrow/fast and wide/slow outflow components, respectively, could naturally account for the appearance of refreshed shocks following (or even coincident with) the wide component's emergence in the afterglow lightcurve. Future high-quality observations should be able to determine whether the nonsteady behavior found in these two objects is a common trait of GRB sources.

APPENDIX

R-BAND FLUXES FROM THE TWO OUTFLOW COMPONENTS

For the narrow/fast jet component, typically $t_{\mathrm{dec,n}}$ is smaller than all the other transition times and $t_{0,\mathrm{n}} < t_{\mathrm{jet},n}$, so there are four interesting regimes of observed frequencies: $\nu > \nu_{0,\mathrm{n}}$; $\quad \nu_{\mathrm{c,n}}(t_{\mathrm{jet,n}}) < \nu < \nu_{0,\mathrm{n}}$; $\quad \nu_{\mathrm{m,n}}(t_{\mathrm{jet,n}}) < \nu <$

$\nu_{c,n}(t_{jet,n}); \quad \nu < \nu_{m,n}(t_{jet,n})$. The corresponding fluxes are

$$\frac{F_{\nu,n}}{F_{\nu,\max,n}} = \begin{cases} (t_{dec,n}/t_{c,n})^{1/6}(t/t_{dec,n})^{11/3} & t < t_{dec,n} \ , \\ (t/t_{c,n})^{1/6} & t_{dec,n} < t < t_{c,n} \ , \\ (t/t_{c,n})^{-1/4} & t_{c,n} < t < t_{m,n} \ , \\ (t_{m,n}/t_{c,n})^{-1/4}(t/t_{m,n})^{-(3p-2)/4} & t_{m,n} < t < t_{jet,n} \ , \\ (t_{m,n}/t_{c,n})^{-1/4}(t_{jet,n}/t_{m,n})^{-(3p-2)/4}(t/t_{jet,n})^{-p} & t > t_{jet,n} \ , \end{cases} \tag{A1}$$

$$\frac{F_{\nu,n}}{F_{\nu,\max,n}} = \begin{cases} (t_{0,n}/t_{m,n})^{1/2}(t_{dec,n}/t_{0,n})^{1/6}(t/t_{dec,n})^{11/3} & t < t_{dec,n} \ , \\ (t_{0,n}/t_{m,n})^{1/2}(t/t_{0,n})^{1/6} & t_{dec,n} < t < t_{0,n} \ , \\ (t/t_{m,n})^{1/2} & t_{0,n} < t < t_{m,n} \ , \\ (t/t_{m,n})^{-3(p-1)/4} & t_{m,n} < t < t_{c,n} \ , \\ (t_{c,n}/t_{m,n})^{-3(p-1)/4}(t/t_{c,n})^{-(3p-2)/4} & t_{c,n} < t < t_{jet,n} \ , \\ (t_{c,n}/t_{m,n})^{-3(p-1)/4}(t_{jet,n}/t_{c,n})^{-(3p-2)/4}(t/t_{jet,n})^{-p} & t > t_{jet,n} \ , \end{cases} \tag{A2}$$

$$\frac{F_{\nu,n}}{F_{\nu,\max,n}} = \begin{cases} (t_{0,n}/t_{m,n})^{1/2}(t_{dec,n}/t_{0,n})^{1/6}(t/t_{dec,n})^{11/3} & t < t_{dec,n} \ , \\ (t_{0,n}/t_{m,n})^{1/2}(t/t_{0,n})^{1/6} & t_{dec,n} < t < t_{0,n} \ , \\ (t/t_{m,n})^{1/2} & t_{0,n} < t < t_{m,n} \ , \\ (t/t_{m,n})^{-3(p-1)/4} & t_{m,n} < t < t_{jet,n} \ , \\ (t_{jet,n}/t_{m,n})^{-3(p-1)/4}(t/t_{jet,n})^{-p} & t > t_{jet,n} \ , \end{cases} \tag{A3}$$

$$\frac{F_{\nu,n}}{F_{\nu,n}(t_{jet,n})} = \begin{cases} (t_{0,n}/t_{jet,n})^{1/2}(t_{dec,n}/t_{0,n})^{1/6}(t/t_{dec,n})^{11/3} & t < t_{dec,n} \ , \\ (t_{0,n}/t_{jet,n})^{1/2}(t/t_{0,n})^{1/6} & t_{dec,n} < t < t_{0,n} \ , \\ (t/t_{jet,n})^{1/2} & t_{0,n} < t < t_{jet,n} \ , \\ (t/t_{jet,n})^{-1/3} & t_{jet,n} < t < t_{m,n} \ , \\ (t_{m,n}/t_{jet,n})^{-1/3}(t/t_{m,n})^{-p} & t > t_{m,n} \ . \end{cases} \tag{A4}$$

It is worth noting at this point that the simple power-law scalings we employ in this paper may not always give an accurate representation of the actual behavior of a real outflow. Possible discrepancies have, in fact, been indicated by the hydrodynamical simulations reported in Granot et al. (2001). For example, the scaling $F_\nu \propto t^{-1/3}$ given in the next-to-last line of equation (A4) appears to differ from the behavior exhibited in Figure 2 of that reference, where the flux at low frequencies is shown to continue rising well past t_{jet}. However, the expressions that are most relevant to the behavior of the optical afterglow seem to be consistent with the results of the numerical simulations.

For the wide/slow jet component, the cooling frequency ν_c is always larger than the characteristic frequency ν_m for typical parameters, so it is always slow cooling. This can be verified in the following analysis. Since the ratio ν_c/ν_m decreases with time before t_{dec} and increases with time after t_{dec}, it reaches its minimum value at t_{dec}, and the condition for always being in slow cooling is $(\nu_c/\nu_m)|_{t_{dec,w}} > 1$. Combining equations (1) and (2), we get

$$(\nu_c/\nu_m)|_{t_{dec,w}} = 3.8\, g^{-2} E_{iso,w,52}^{-2/3} \epsilon_{B,-1}^{-2} \epsilon_{e,-1}^{-2} n_0^{-4/3} (\eta_w/10)^{-8/3} \ . \tag{A5}$$

For the typical parameter ranges described at the end of this Appendix, $(\nu_c/\nu_m)|_{t_{dec,w}} \sim 5\times10^{-5} - 2\times10^9$, which shows that $(\nu_c/\nu_m)|_{t_{dec,w}} > 1$ for most parameter values. This inequality is violated only when all the relevant parameters are close to their maximum values, which is not a typical situation. If, in addition, $\nu_{c,w}(t_{jet,w}) > \nu_{m,w}(t_{dec,w})$ is also satisfied (which is again true for most parameter values), then there are five interesting frequency regimes: $\nu > \nu_{c,w}(t_{dec,w})$, $\nu_{c,w}(t_{jet,w}) < \nu < \nu_{c,w}(t_{dec,w})$, $\nu_{m,w}(t_{dec,w}) < \nu < \nu_{c,w}(t_{jet,w})$, $\nu_{m,w}(t_{jet,w}) < \nu < \nu_{m,w}(t_{dec,w})$, and $\nu < \nu_{m,w}(t_{jet,w})$. The corresponding fluxes are

$$\frac{F_{\nu,w}}{F_{\nu,w}(t_{dec,w})} = \begin{cases} (t_{c,w}/t_{dec,w})^2(t/t_{c,w})^3 & t < t_{c,w} \ , \\ (t/t_{dec,w})^2 & t_{c,w} < t < t_{dec,w} \ , \\ (t/t_{dec,w})^{-(3p-2)/4} & t_{dec,w} < t < t_{jet,w} \ , \\ (t_{jet,w}/t_{dec,w})^{-(3p-2)/4}(t/t_{jet,w})^{-p} & t > t_{jet,w} \ , \end{cases} \tag{A6}$$

$$\frac{F_{\nu,w}}{F_{\nu,w}(t_{dec,w})} = \begin{cases} (t/t_{dec,w})^3 & t < t_{dec,w} \ , \\ (t/t_{dec,w})^{-3(p-1)/4} & t_{dec,w} < t < t_{c,w} \ , \\ (t_{c,w}/t_{dec,w})^{-3(p-1)/4}(t/t_{c,w})^{-(3p-2)/4} & t_{c,w} < t < t_{jet,w} \ , \\ (t_{c,w}/t_{dec,w})^{-3(p-1)/4}(t_{jet,w}/t_{c,w})^{-(3p-2)/4}(t/t_{jet,w})^{-p} & t > t_{jet,w} \ , \end{cases} \tag{A7}$$

$$\frac{F_{\nu,w}}{F_{\nu,w}(t_{dec,w})} = \begin{cases} (t/t_{dec,w})^3 & t < t_{dec,w} \ , \\ (t/t_{dec,w})^{-3(p-1)/4} & t_{dec,w} < t < t_{jet,w} \ , \\ (t_{jet,w}/t_{dec,w})^{-3(p-1)/4}(t/t_{jet,w})^{-p} & t > t_{jet,w} \ , \end{cases} \tag{A8}$$

$$\frac{F_{\nu,\mathrm{w}}}{F_{\nu,\mathrm{max,w}}} = \begin{cases} (t_{\mathrm{dec,w}}/t_{\mathrm{m,w}})^{1/2}(t/t_{\mathrm{dec,w}})^3 & t < t_{\mathrm{dec,w}} \ , \\ (t/t_{\mathrm{m,w}})^{1/2} & t_{\mathrm{dec,w}} < t < t_{\mathrm{m,w}} \ , \\ (t/t_{\mathrm{m,w}})^{-3(p-1)/4} & t_{\mathrm{m,w}} < t < t_{\mathrm{jet,w}} \ , \\ (t_{\mathrm{jet,w}}/t_{\mathrm{m}})^{-3(p-1)/4}(t/t_{\mathrm{jet,w}})^{-p} & t > t_{\mathrm{jet,w}} \ , \end{cases} \tag{A9}$$

$$\frac{F_{\nu,\mathrm{w}}}{F_{\nu,\mathrm{w}}(t_{\mathrm{jet},w})} = \begin{cases} (t_{\mathrm{dec,w}}/t_{\mathrm{jet,w}})^{1/2}(t/t_{\mathrm{dec,w}})^3 & t < t_{\mathrm{dec,w}} \ , \\ (t/t_{\mathrm{jet},w})^{1/2} & t_{\mathrm{dec,w}} < t < t_{\mathrm{jet,w}} \ , \\ (t/t_{\mathrm{jet,w}})^{-1/3} & t_{\mathrm{jet,w}} < t < t_{\mathrm{m,w}} \ , \\ (t_{\mathrm{m,w}}/t_{\mathrm{jet}})^{-1/3}(t/t_{\mathrm{m,w}})^{-p} & t > t_{\mathrm{m,w}}. \end{cases} \tag{A10}$$

If, on the other hand, $\nu_{\mathrm{c,w}}(t_{\mathrm{jet,w}}) < \nu_{\mathrm{m,w}}(t_{\mathrm{dec,w}})$, then there is an additional possible shape for the lightcurve when $\nu_{\mathrm{c,w}}(t_{\mathrm{jet,w}}) < \nu < \nu_{\mathrm{m,w}}(t_{\mathrm{dec,w}})$:

$$\frac{F_{\nu,\mathrm{w}}}{F_{\nu,\mathrm{max,w}}} = \begin{cases} (t_{\mathrm{dec,w}}/t_{\mathrm{m,w}})^{1/2}(t/t_{\mathrm{dec,w}})^3 & t < t_{\mathrm{dec,w}} \ , \\ (t/t_{\mathrm{m,w}})^{1/2} & t_{\mathrm{dec,w}} < t < t_{\mathrm{m,w}} \ , \\ (t/t_{\mathrm{m,w}})^{-3(p-1)/4} & t_{\mathrm{m,w}} < t < t_{\mathrm{c,w}} \ , \\ (t_{\mathrm{c,w}}/t_{\mathrm{m}})^{-3(p-1)/4}(t/t_{\mathrm{c,w}})^{-(3p-2)/4} & t_{\mathrm{c,w}} < t < t_{\mathrm{jet,w}} \ , \\ (t_{\mathrm{c,w}}/t_{\mathrm{m}})^{-3(p-1)/4}(t_{\mathrm{jet,w}}/t_{\mathrm{c,w}})^{-(3p-2)/4}(t/t_{\mathrm{jet,w}})^{-p} & t > t_{\mathrm{jet,w}} \ . \end{cases} \tag{A11}$$

In this work we are interested in the R-band spectral regime, so we compare the characteristic frequencies at the main spectral transition times with a typical optical frequency ν_{R}. In particular, at $t_{\mathrm{dec,w}}$,

$$\nu_{\mathrm{c,w}}(t_{\mathrm{dec,w}}) = 5.2 \times 10^{13} \, E_{\mathrm{iso,w},52}^{-2/3} \epsilon_{B,-1}^{-3/2} n_0^{-5/6} (\eta_{\mathrm{w}}/10)^{4/3} \ \mathrm{Hz} \ , \tag{A12}$$

$$\nu_{\mathrm{c,n}}(t_{\mathrm{dec,w}}) = \begin{cases} \nu_{\mathrm{c,w}}(t_{\mathrm{dec,w}}) \left(\frac{E_{\mathrm{iso,w}}}{E_{\mathrm{iso,n}}}\right)^{1/2} & t_{\mathrm{dec,w}} < t_{\mathrm{jet,n}} \ , \\ \nu_{\mathrm{c,n}}(t_{\mathrm{jet,n}}) & t_{\mathrm{dec,w}} > t_{\mathrm{jet,n}} \ , \end{cases} \tag{A13}$$

$$\nu_{\mathrm{m,w}}(t_{\mathrm{dec,w}}) = 1.4 \times 10^{13} \, g^2 \epsilon_{e,-1}^2 \epsilon_{B,-1}^{1/2} n_0^{1/2} (\eta_{\mathrm{w}}/10)^4 \ \mathrm{Hz} \ , \tag{A14}$$

$$\nu_{\mathrm{m,n}}(t_{\mathrm{dec,w}}) = \begin{cases} \nu_{\mathrm{m,w}}(t_{\mathrm{dec,w}}) \left(\frac{E_{\mathrm{iso,w}}}{E_{\mathrm{iso,n}}}\right)^{-1/2} & t_{\mathrm{dec,w}} < t_{\mathrm{jet,n}} \ , \\ \nu_{\mathrm{m,n}}(t_{\mathrm{jet,n}}) \left(\frac{E_{\mathrm{iso,w}}}{E_{\mathrm{iso,n}}}\right)^{-2/3} (\eta_{\mathrm{w}}\theta_{\mathrm{j,n}})^{16/3} & t_{\mathrm{dec,w}} > t_{\mathrm{jet,n}} \ . \end{cases} \tag{A15}$$

We also have

$$\nu_{\mathrm{c}}(t_{\mathrm{jet}}) = 1.6 \times 10^{14} \, E_{\mathrm{iso},52}^{-2/3} \epsilon_{B,-1}^{-3/2} n_0^{-5/6} \theta_{\mathrm{j,-1}}^{-4/3} \ \mathrm{Hz} \ , \tag{A16}$$

$$\nu_{\mathrm{m}}(t_{\mathrm{jet}}) = 1.4 \times 10^{13} \, g^2 \epsilon_{e,-1}^2 \epsilon_{B,-1}^{1/2} n_0^{1/2} \theta_{\mathrm{j,-1}}^{-4} \ \mathrm{Hz} \ . \tag{A17}$$

We adopt as typical parameter ranges $p \sim 1.5 - 3$, $n_0 = 0.3 - 30$, $\epsilon_e = 0.005 - 0.3$, $\epsilon_B = 0.001 - 0.1$, $\theta_{\mathrm{j,n}} \sim 0.05 - 0.1$, $\theta_{\mathrm{j,w}} \sim 0.1 - 0.3$, $E_{\mathrm{n}} \sim E_{\mathrm{w}} \sim 10^{50} - 10^{51}$ ergs (Panaitescu & Kumar 2002), $\eta_{\mathrm{n}} \sim 10^2$, and $\eta_{\mathrm{w}} \sim 10$. For this set of parameters we find that the following inequalities are always obeyed: $\nu_{\mathrm{m,n}}(t_{\mathrm{dec,n}}) > \nu_{\mathrm{R}} > \nu_{\mathrm{m,n}}(t_{\mathrm{jet},n})$, $\nu_{\mathrm{R}} > \nu_{\mathrm{m,n}}(t_{\mathrm{dec,w}})$, and $\nu_{\mathrm{R}} > \nu_{\mathrm{m,w}}(t_{\mathrm{dec,w}})$. The observation frequency ν_{R} can be larger or smaller than ν_{c} for both components at $t_{\mathrm{jet,n}}$ and $t_{\mathrm{dec,w}}$. However, for the parameter combinations employed in the plots shown in this paper, $\nu_{\mathrm{c,n}}(t_{\mathrm{jet,n}}) > \nu_{\mathrm{R}} > \nu_{\mathrm{m,n}}(t_{\mathrm{jet,n}})$ and $\nu_{\mathrm{c,w}}(t_{\mathrm{dec,w}}) > \nu_{\mathrm{R}} > \nu_{\mathrm{m,w}}(t_{\mathrm{dec,w}})$. Since ν_m and ν_m/ν_c decrease with time (see eqs. [7] and [8]), the inequalities $\nu_{\mathrm{c}} > \nu_{\mathrm{m}}$ and $\nu_{\mathrm{R}} > \nu_{\mathrm{m}}$ continue to apply after the specified times. For the narrow component $\nu_{\mathrm{c,n}} > \nu_{\mathrm{R}} > \nu_{\mathrm{m,n}}$ also continues to apply since (under the assumptions underlying eq. [8]) $\nu_{\mathrm{c,n}}$ remains constant for $t > t_{\mathrm{jet,n}}$. However, $\nu_{\mathrm{c,w}}$ decreases with time after $t_{\mathrm{dec,w}}$ and could potentially fall below ν_{R} before its value becomes frozen at $t_{\mathrm{j,w}}$. The foregoing arguments imply that the frequency regimes corresponding to equations (A4), (A9), (A10), and (A11) would typically not be relevant.

REFERENCES

Beloborodov, A. M. 2000, ApJ, 539, L25
Berger, E., Kulkarni, S., & Frail, D. A. 2003a, ApJ, 590, 379
Berger, E., et al. 2003b, Nature, 426, 154
Blandford, R. D., & McKee, C. 1976, Phys. Fluids, 19, 1130
Bloom, J. S., Frail, D. A., & Kulkarni, S. R. 2003, ApJ, 594, 674
Cannizzo, J. K., Gehrels, N., & Vishniac, E. T. 2004, ApJ, 601, 380
Fox, D. W., et al. 2003, Nature, 422, 284
Frail, D. A., et al. 2000, ApJ, 538, L129
Frail, D. A., et al. 2001, ApJ, 562, L55
Fynbo, J. P. U., et al. 2004, ApJ, 609, 962
Granot, J., Miller, M., Piran, T., Suen, W. M., & Hughes, P. A. 2001, in Gamma-Ray Bursts in the Afterglow Era, ed. E. Costa, F. Frontera, & J. Hjorth (Berlin: Springer), 312
Granot, J., Nakar, E., & Piran, T. 2003, Nature, 426, 138
Granot, J., Panaitescu, A., Kumar, P., & Woosley, S. E. 2002, ApJ, 570, L61
Granot, J., Ramirez-Ruiz, E., & Loeb, A. 2005, ApJ, 618, 413
Heise, J. 2003, in AIP Conf. Proc. 662, Gamma-Ray Burst and Afterglow Astronomy 2001, ed. G. R. Ricker & R. K. Vanderspek (Melville: AIP), 229
Hjorth, J., et al. 2003, Nature, 423, 847
Huang, Y. F., Wu, X. F., Dai, Z. G., Ma, H. T., & Lu, T. 2004, ApJ, 605, 300
Khokhlov, A. M., Höflich, P. A., Oran, E. S., Wheeler, J. C., Wang, L., & Chtchelkanova, Y. 1999, ApJ, 524, L107
Kippen, M., Woods, P. M., Heise, J., In't Zand, J. J. M., Briggs, M. S., & Preece, R. D. 2003, in AIP Conf. Proc. 662, Gamma-Ray Burst and Afterglow Astronomy 2001, ed. G. R. Ricker & R. K. Vanderspek (Melville: AIP), 244
Kobayashi, S., & Sari, R. 2001, ApJ, 551, 934
Kobayashi, S., & Zhang, B. 2003, ApJ, 582, L75
Königl, A. 2004, in AIP Conf. Proc. 727, Gamma-Ray Bursts: 30 Years of Discovery, ed. E. E. Fenimore & M. Galassi (Melville: AIP), 257
Kumar, P., & Granot, J. 2003, ApJ, 591, 1075
Kumar, P., & Piran, T. 2000a, ApJ, 532, 286
Kumar, P., & Piran, T. 2000b, ApJ, 535, 152
Lazzati, D., Rossi, E., Covino, S., Ghisellini, G., & Malesani, D. 2002, A&A, 396, L5
Levinson, A., & Eichler, D. 1993, ApJ, 418, 386
Liang, E. W., & Dai, Z. G. 2004, ApJ, 608, L9
Lipkin, Y. M., et al. 2004, ApJ, 606, 381
Mészáros, P. 2002, ARAA, 40, 137
Nakar, E., & Oren, Y. 2004, ApJ, 602, L97
Nakar, E., & Piran, T. 2002, ApJ, 572, L139

Nakar, E., & Piran, T. 2003, ApJ, 598, 400
Nakar, E., Piran, T., & Granot, J. 2002, ApJ, 579, 699
Nakar, E., Piran, T., & Granot, J. 2003, NewA, 8, 495
Panaitescu, A., & Kumar, P. 2002, ApJ, 571, 779
Panaitescu, A., Mészáros, P., & Rees, M. J. 1998, ApJ, 503, 314
Pedersen, H., et al. 1998, ApJ, 496, 311
Piran, T. 1999, Phys. Rep. 314, 575
Piran, T., Nakar, E., & Granot, J. 2004, in AIP Conf. Proc. 727, Gamma-Ray Bursts: 30 Years of Discovery, ed. E. E. Fenimore & M. Galassi (Melville: AIP), 181
Price, P.A., et al. 2003, Nature, 423, 824
Ramirez-Ruiz, E., Celotti, A., & Rees, M. J. 2002, MNRAS, 337, 1349
Rees, M. J., & Mészáros, P. 1994, ApJ, 430, L93
Rhoads, J. 1999, ApJ, 525, 737
Rossi, E., Lazzati, D., & Rees, M. J. 2002, MNRAS, 332, 945
Sari, R. 1997, ApJ, 489, L37
Sari, R., & Mészáros, P. 2000, ApJ, 535, L33
Sari, R., & Piran, T. 1995, ApJ, 455, L143
Sari, R., & Piran, T. 1999a, ApJ, 520, 641
Sari, R., & Piran, T. 1999b, A&A Supl. Ser., 138, 537
Sari, R., Piran, T., & Halpern J. P., 1999, ApJ, 519, L17
Sari, R., Piran, T., & Narayan, R. 1998, ApJ, 497, L17
Sheth, K., et al. 2003, ApJ, 595, L33
Soderberg, A. M., et al. 2004, ApJ, 606, 994
Starling, R. L. C., Wijers, R. A. M. J., Hughes, M. A., Tanvir, N. R., Vreeswijk, P. M., Rol, E., & Salamanca, I. 2005, MNRAS, in press (astro-ph/0501120)
Taylor, G.B., Frail, D.A., Berger, E., & Kulkarni, S.R. 2004, ApJ, 609, L1
Uemura, M., Kato, T., Ishioka, R., & Yamaoka, H. 2003, PASJ, 55L, 31
van Putten, M. H. P. M., & Levinson, A. 2003, ApJ, 584, 937
Vlahakis, N., Peng, F., & Königl, A. 2003, ApJ, 594, L23
Willingale, R., Osborne, J. P., O'Brien, P. T., Ward, M. J., Levan, A., & Page, K. L. 2004, MNRAS, 349, 31
Yamazaki, R., Ioka, K., & Nakamura, T. 2002, ApJ, 571, L31
Yamazaki, R., Ioka, K., & Nakamura, T. 2004, ApJ, 606, L33
Yost, S. A., Harrison, F. A., Sari, R., & Frail, D. A. 2003, ApJ, 597, 459
Zhang, B., Dai, X., Lloyd-Ronning, N. M., & Mészáros, P. 2004, ApJ, 601, L119
Zhang, B., & Mészáros, P. 2002, ApJ, 571, 876
Zhang, W., Woosley, S. E. & Heger, A. 2004, ApJ, 608, 365